Contribution from the Department of Chemistry and Materials Science Center, Cornell University, Ithaca, New York, 14853, and from Queen Mary College, University of London, London E1 4NS, Great Britain

# Comparative Bonding Study of Conical Fragments

MIHAI ELIAN, MAYNARD M. L. CHEN, D. MICHAEL P. MINGOS, and ROALD HOFFMANN*

*Received January 7, 1976* AIC600224

A detailed construction of the frontier orbitals of $M(CO)_3$ and M(benzene) fragments leads to a general analysis of $M(CO)_3$ and $M(CH)_n$, $n$ = 3–8. The number, symmetry properties, energy, and extent in space of these frontier orbitals determine their interaction with other ligands completing the metal coordination sphere. An overlap analysis of the bonding capabilities of $M(CO)_3$, M(benzene), and M(cyclopentadienyl) leads to the conclusion that in interaction with another metal $M(C_6H_6)$ or MCp has a stronger $\sigma$ interaction, but $M(CO)_3$ is better at $\pi$ bonding. In interaction with a main-group probe oxidation state effects appear to dominate. Structural information on pertinent replacement pairs is surveyed to evaluate the validity of these theoretical conclusions. The bending of hydrogens out of the carbon plane in $M(CH)_n$ complexes is traced to $\pi$ interactions and a reorientation of the ring $\pi$ orbitals for better overlap. The result is bending toward the metal for large $n$ and away from the metal for small $n$. Pyramidality deformations in $M(CO)_nL_m$ are predicted in response to the donor capability of L.

Between a set of three carbonyls and the cyclic polyene or polyenyl systems $(CH)_n$, $n$ = 3–8, one has covered the majority of ligand types in known transition metal complexes. These ligands are often interchangeable. Our interest is in the obvious similarities and the subtle differences of $M(CO)_3$ and $M(CH)_n$ fragments and the consequences of these similarities and differences on their bonding capability. We begin with a detailed comparison of $M(CO)_3$, **1**, with $M(\eta^6\text{-}C_6H_6)$, **2**, and

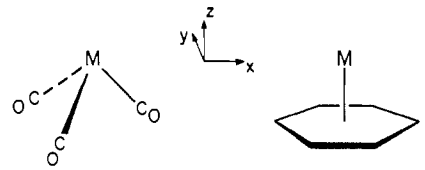


1 2

then turn to the general features of $M(CH)_n$ fragments. At the end of the paper we attempt to correlate our theoretical conclusions with the available structural information on $M(CO)_3$, M(arene), and M(Cp) complexes.

## Theoretical Comparison of the $M(CO)_3$ and M(benzene) Fragments

Interaction diagrams for the formation of **1** and **2** from a metal atom and three carbonyls or a benzene are shown in Figure 1. These diagrams, as well as the other computations referred to below, are derived from extended Hückel calculations for M = Mn, with parameters and geometrical details given in the Appendix. Only those levels which figure in our discussion are shown.

The differences between the frontier orbitals of **1** and **2** are ones of energy (indicated in Figure 1), of extent in space, and of shape (to be discussed below). The origin of these differences lies in the low-lying empty orbitals of the carbonyls, which find no counterpart in benzene. The following specific comparisons may be made.

1. The similarities of fragments **1** and **2** are the expected ones. For a $d^6$ configuration both **1** and **2** have a set of three low-lying acceptor orbitals of a + e symmetry, marked[1] "hy", $xz$, and $yz$ in Figure 1. The shapes of these orbitals will be discussed below. Here it suffices to say that they are directed away from the $(CO)_3$ or $C_6H_6$ and may be adequately described as a set of three hybrids **3**. They are ideally prepared to interact with another six-electron donor system.

2. The first difference between $M(CO)_3$ and $M(C_6H_6)$ is in the energy of the $z^2$ orbital. In **1** $z^2$ is stabilized by a dominant interaction with an $a_1$ combination[2] of $(CO)_3$, while


3

in **2** $z^2$ is destabilized by a filled $a_1$. It is interesting to note that our calculations indicate that in this destabilization the lowest benzene $\pi$ orbital, $a_{2u}$, is not as important as a still lower energy radial type $\sigma$ orbital of $a_{1g}$ symmetry.[3] The reason for this is that at a typical metal–benzene distance the 2p orbitals of the benzene ring lie approximately in the nodal plane of the $z^2$ orbital. To the extent that the $z^2$ orbital in **1** is stabilized by mixing in the carbonyl $\pi^*$ $a_1$ combination there will be a net transfer of electrons from the metal to $(CO)_3$, providing $z^2$ is occupied.

3. In both fragments the $xy$ and $x^2 - y^2$ orbitals are slightly stabilized. In **2** symmetry restricts interaction to the LUMO's of benzene, $e_{2u}$. In **1** mixing is allowed with all e orbitals. The most important interaction seems to be with 2 e, derived from the carbonyl $\pi^*$ set. The calculation shows larger overlap in the $(CO)_3$ case, which would again lead to greater stabilization and metal to ligand charge transfer when these orbitals are filled. It should be noted that in $M(CO)_3$ there is some mixing of the $(x^2 - y^2, xy)$ and $(xz, yz)$ sets.

4. Metal $xz$ and $yz$ are destabilized by filled orbitals of e symmetry. A concomitant effect is the mixing in of $x$ and $y$ orbitals with a phase such that hybrids pointing away from the $(CO)_3$ or $C_6H_6$ are produced.[4] In **4** and **5** are shown contour diagrams of one of these orbitals. In $M(CO)_3$ there is supplemental mixing with unfilled carbonyl orbitals, so that the d character of the orbitals we label $xz$ and $yz$ is somewhat reduced. Also the extent of hybridization with $x$ and $y$ is greater in $M(CO)_3$. The left–right asymmetry of **4** is a consequence of the mixing with $xy$ and $x^2 - y^2$ mentioned above.

5. The orbital labeled "hy" (for hybrid) shows some significant differences in the two fragments. In **2** it is nearly a pure hybrid of s and $z$ while in **1** there is added some $z^2$ character and some delocalization to the $(CO)_3$. The detailed breakdown of the electron density in this $a_1$ orbital is given in Table I. A detailed rationale of the composition of these orbitals can be given by utilizing higher order perturbation theory.[5] The salient features of the analysis are the following. In $M(C_6H_6)$ there is a second-order mixing of metal s and $z$ through their mutual overlap with the benzene $a_{2u}$. The benzene orbital does not itself mix in because the system of s, $z$, and $a_{2u}$ is similar to an allylic $\pi$ system, with s playing

* To whom correspondence should be addressed at Cornell University.

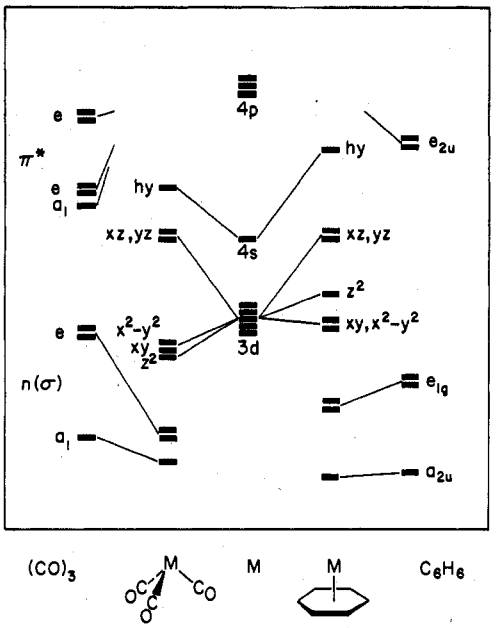


**Figure 1.** Interaction diagrams for the construction of the orbitals of $M(CO)_3$ and $M(C_6H_6)$ from the metal orbitals (at center) and the ligand orbitals (at left and right). The resulting fragment MO's are labeled according to their metal character.

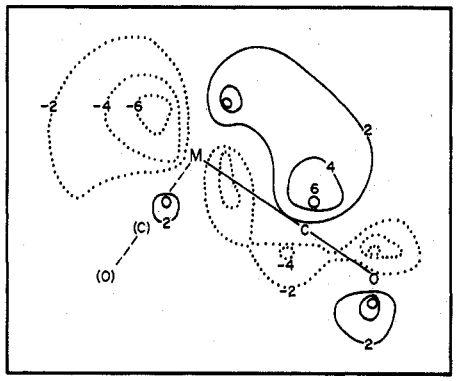

4

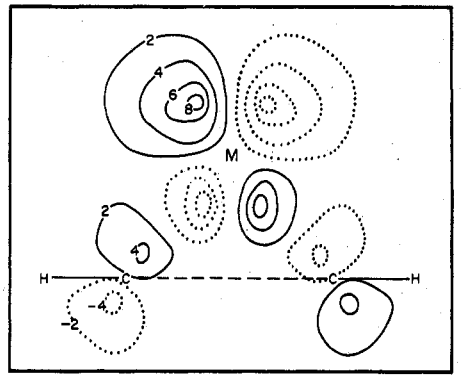

5

the role of orbital 1, $a_{2u}$ orbital 2, and $z$ orbital 3. The middle-energy orbital of an allylic system has little or no density at the central orbital, even though one can think of that orbital as coupling centers 1 and 3. In $M(CO)_3$ the lowest vacant $a_1$ orbital of $(CO)_3$ dominates the coupling pattern, both taking electron density from s and mixing $z^2$ into s. The

**Table I.** Electron Density in "hy" Orbital, in %

| Orbital | Ligand(s) | | |
|---|---|---|---|
| | $(CO)_3$ | $C_6H_6$ | $C_5H_5$ |
| s | 21 | 52 | 54 |
| $z$ | 34 | 45 | 44 |
| $z^2$ | 18 | 0 | 0 |
| Ligand(s) | 27 | 3 | 1 |

**Table II.** Transformation Properties of $(CH)_n$ $\pi$ and Metal Orbitals

| $n$ | $(CH)_n$ | Metal d |
|---|---|---|
| 3 | $a_1 + e$ | $a_1 + 2e$ |
| 4 | $a_1 + e + b_2$ | $a_1 + e + b_1 + b_2$ |
| 5 | $a_1 + e_1 + e_2$ | $a_1 + e_1 + e_2$ |
| 6 | $a_1 + e_1 + e_2 + b_1$ | $a_1 + e_1 + e_2$ |
| 7 | $a_1 + e_1 + e_2 + e_3$ | $a_1 + e_1 + e_2$ |
| 8 | $a_1 + e_1 + e_2 + e_3 + b_1$ | $a_1 + e_1 + e_2$ |

differing shapes of the hy orbital are shown in contour diagrams **6** and **7**.

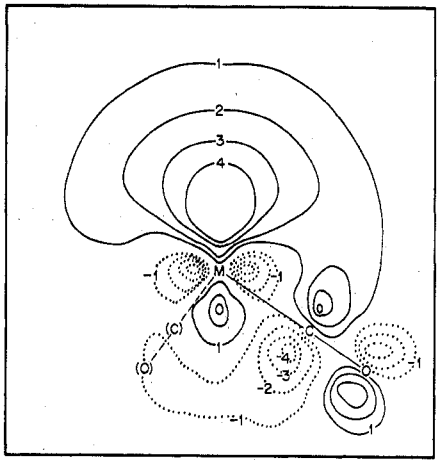

6

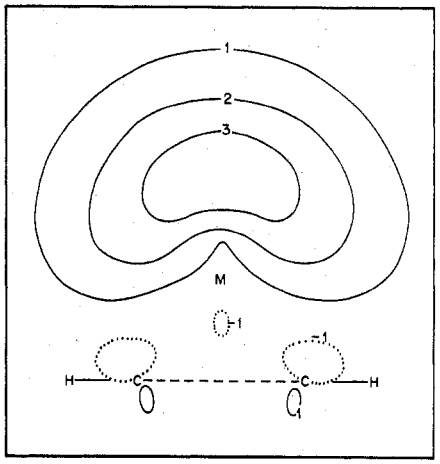

7

Though we have dwelled upon some of the differences between the $M(CO)_3$ and $M(C_6H_6)$ fragments, we urge the reader to view these differences as minor perturbations superimposed on a basically similar pattern. $M(CO)_3$, $M(C_6H_6)$, and M'(Cp), which we will discuss later, can be termed *isolobal*. By this word we mean to imply that the number, symmetry properties, extent in space and energy of the frontier

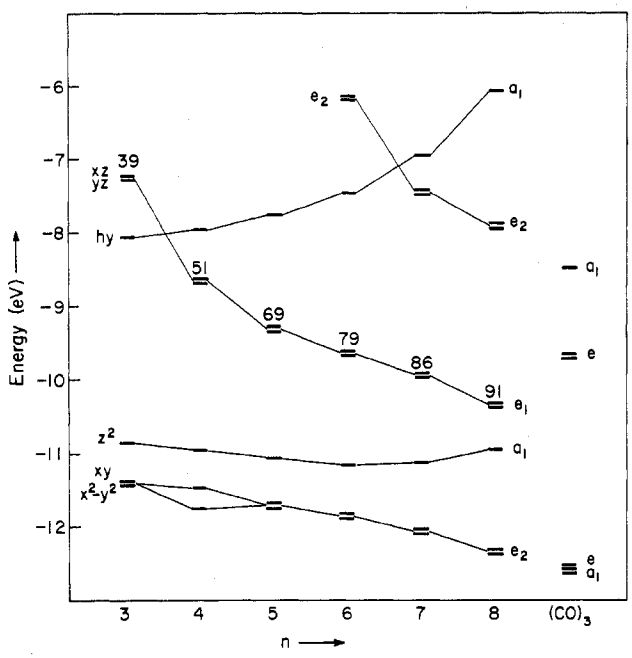


**Figure 2.** Frontier orbitals of $M(CH)_n$, $n = 3$–8, and $M(CO)_3$. For the $e_1$ orbital the percent electron density on the metal is indicated by a number. For $n = 3$ the $e_1$ and $e_2$ labels do not apply–both levels are e. For $n = 4$ the level set which is $e_2$-like is nondegenerate.

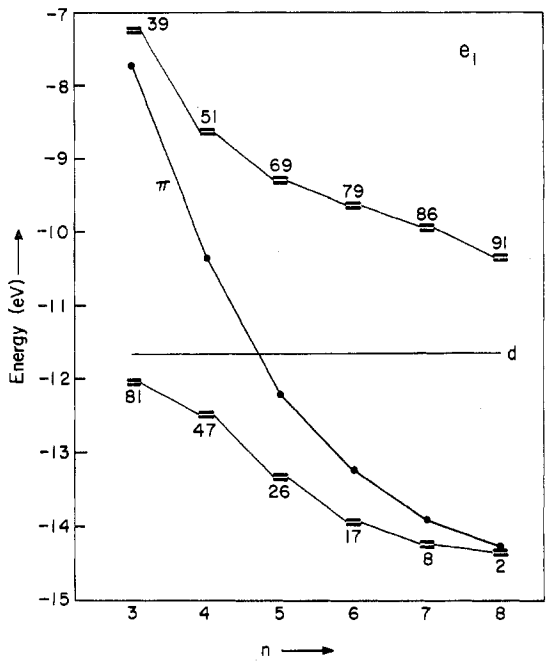


**Figure 3.** Construction of the $e_1$ frontier orbitals from the interaction of a variable-energy $C_nH_n$ $e_1$ and a fixed-energy $xz$, $yz$ set. $\pi$ labels the energy of the $e_1$ set in the cyclopolyene. The numbers are percent metal character.

orbitals of the fragments are similar—not identical, but similar.

The above discussion has correlated the frontier orbitals of $M(CO)_3$ and $M(C_6H_6)$ fragments. What matters, of course, is the way that the resemblance or dissimilarity of these fragments is translated into the manner in which they bind to some other ligand. We will return to a comparison of the relative bonding capabilities of the two fragments later. At this point it is appropriate to enlarge our discussion to include other $M(CH)_n$ species.

### Molecular Orbitals of Other $M(CH)_n$ Fragments

The known cyclopolyene or cyclopolyenyl rings found in transition metal complexes range in size from 3 to 8.[6] The polyene orbitals and their interactions with transition metal atoms are well-known, so that to some extent we run the risk of repeating in this section what is common knowledge.[6–8]

In the reduced $C_{nv}$ symmetry the $\pi$ orbitals of planar $(CH)_n$ rings and the atomic orbitals of a transition metal transform as shown in Table II. The metal s and p orbitals subduce in each case the $2\ a_1 + e$ representations. Of course, it is the cylindrical $C_{\infty v}$ pseudosymmetry which is more important than the actual $C_{nv}$ symmetry. Thus the metal d orbitals are $\sigma + \pi + \delta$ in all cases, and the cyclopolyene orbitals can be reclassified accordingly. A perfect match for the metal d orbitals is found in the $a_1 + e_1 + e_2$ orbitals of a cyclopolyene for $n \geq 5$. From that point on, the differences among the various $M(CH)_n$ species are only quantitative, depending on the relative energies of the cyclopolyene and metal orbitals.

All of the interaction diagrams are in fact qualitatively alike, as shown in Figure 2. This illustrates the frontier orbitals of $Mn(CH)_n$, along with those of $Mn(CO)_3$ for comparison. In the $Mn(CH)_n$ geometries which we utilized, the Mn–C distance was kept fixed at 2.19 Å. In all $M(CH)_n$ we recognize a cluster of three relatively low-lying orbitals, mainly on the metal, composed of $z^2$, $xy$, and $x^2 - y^2$. These are characteristic of an octahedral fragment. At higher energy (at least for low $n$) there is an $a_1 + e_1$ set of hybrids directed away from the metal. For high $n$ there comes in an $e_2$ orbital, primarily localized on the ligands. We proceed to detailed examination of the various frontier orbitals.

The low-lying $xy$ and $x^2 - y^2$ set, of $e_2$ symmetry, moves to lower energy with increasing $n$. At the same time its delocalization to the ligands increases. The energy and delocalization trends are of course a reflection of increased interaction with a $(CH)_n$ $e_2$ orbital, of $\delta$ pseudosymmetry. For $n \geq 5$ such a $\pi$ orbital is present, at increasingly lower energy for higher $n$. Note for these higher $n$ values the presence in the diagram of the higher $e_2$ combination, metal–ligand antibonding. For an account of the role of the $e_2$ orbitals the reader is directed to the important contributions of Green, de Liefde Meijer, and their co-workers.[8]

Not far from the $xy$, $x^2 - y^2$ set lies an $a_1$ orbital, which varies relatively little in energy and composition with $n$. Both this $z^2$ orbital and hy are highly localized on the metal, 92–98% on the metal over the entire range of $n$. The energy of hy changes as a result of a change in sp hybridization, from 59% s and 39% $z$ at $n = 3$ to 40% s and 56% $z$ at $n = 8$.

The most dramatic variation is in the $e_1$ or $\pi$ orbitals. They drop in energy with $n$, become more localized on the metal, and mix in less $x$ and $y$ character. What is happening is made explicit by Figure 3. It shows the energy of the $(CH)_n$ $e_1$ orbitals as a function of $n$, as well as the (assumed!) straight-line energy of the metal d orbitals. The two $e_1$ orbitals which result from the interaction are very clearly the result of an "avoided crossing" and a strongly avoided one at that. The lower $e_1$ set, which was not drawn in Figure 2, starts out as mainly metal and ends up as primarily ligand. The upper $e_1$ set, metal–ligand antibonding, is primarily ligand at low $n$ and is changed continuously to heavily metal character at high $n$. The change in hybridization can also be explicated by application of second-order perturbation theory.

A comparison with $M(CO)_3$ shows that for no $n$ can the $(CH)_n$ hy orbital match the acceptor capability of the corresponding $M(CO)_3$ orbital—the latter is always at lower energy. This is for interactions with a main-group probe. The $e_1$ $xz$, $yz$ set may play either a donor or an acceptor role, depending on the $d^n$ configuration. If $e_1$ is empty, then in $M(CH)_n$ it can achieve energetic parity with $M(CO)_n$ or even surpass it in acceptor capability, for $n \geq 6$. If $e_1$ is occupied, then it becomes a better donor than $M(CO)_n$ for $n \leq 5$.

Table III. Overlaps between $ML_n$ Acceptor Orbitals and NO and $MnH_3$ Probe Orbitals

| | Overlaps with NO | | Overlaps with $MnH_3$ | |
|---|---|---|---|---|
| | ⟨hy\|n⟩ | ⟨xz\|$\pi_x$*⟩ | ⟨hy\|hy⟩ | ⟨xz\|xz⟩ |
| $M(CO)_3$ | 0.178 | 0.133 | 0.622 | 0.205 |
| $M(C_6H_6)$ | 0.134 | 0.151 | 0.820 | 0.171 |

Table IV. Metal-Probe Overlaps

| $ML_n$ metal orbital | N | | Mn | | |
|---|---|---|---|---|---|
| | 2s | $2p_z$ | 4s | $4p_z$ | $3d_{z^2}$ |
| 4s | 0.30 | 0.02 | 0.59 | 0.50 | 0.02 |
| $4p_z$ | 0.44 | 0.01 | 0.50 | 0.24 | 0.03 |
| $3d_{z^2}$ | 0.24 | 0.17 | 0.02 | 0.03 | 0.06 |

## Relative Bonding Capabilities of $M(CO)_3$ and $M(C_6H_6)$ Fragments

We now return to our primary objective of assessing the relative interactions of $M(CH)_n$ and $M(CO)_3$ with external ligands. $M(CO)_3$ and $M(C_6H_6)$, whose orbital structure has been analyzed in detail above, will serve as a departure point. Of course there is an infinite variety of ligands which can bind to these fragments. The common feature that otherwise disparate potential bonding partners for $ML_n$ will carry is a donor function. This will interact strongly with the acceptor orbitals of $M(CO)_3$ or $M(C_6H_6)$. Which of the six frontier orbitals serve as donors or acceptors of course depends on the d-electron configuration. The most common 18-electron cases will be $d^6$–$d^{10}$, so that the acceptor orbitals will be hy, *xz*, and *yz*.

One of the several ways that we explored for judging the bonding capability of the $ML_n$ moiety was to calculate overlaps between the hy, *xz*, and *yz* orbitals and appropriate symmetry group orbitals of a bonding partner. It became apparent that it was important to distinguish between main and transition group partners. As an example of the former, we chose a nitrosyl group, with its nitrogen atom placed 1.71 Å from the metal atom.[9] This ligand has a well-developed lone pair, denoted as *n*, and a set of low-lying $\pi^*$ orbitals. As a transition metal bonding probe we chose a hypothetical $MnH_3$ fragment placed 2.9 Å away from M. The $MnH_3$ has $\sigma$ and $\pi$ orbitals quite analogous to those of the $ML_n$ system we have discussed. Table III shows the computed overlaps between hy, *xz*, and *yz* and the corresponding symmetry probe orbitals.

The ordering of the interactions in Table III merits explication. In interpreting the various overlaps with hy, it is useful first to recall (Table I) that in $M(CO)_3$ hy is a mixture of metal s, *z*, and $z^2$ and is somewhat delocalized to the carbonyl groups. In $M(C_6H_6)$ hy is a nearly pure mixture of metal s and *z*. Table IV lists the computed overlaps between metal s, *z*, $z^2$, and various $\sigma$ orbitals of the probe.

Consider first the $ML_n$–N overlap. The metal s and *z* orbitals are so diffuse that they overlap nearly equally with both the positive and negative lobes of N *z*. This accounts for the small overlaps with N *z*. Metal $z^2$, reasonably contracted, has significant overlaps with the main-group probe s and *z* orbitals. Since the distinction between $M(CO)_3$ and $M(C_6H_6)$ is primarily that the former carries $z^2$ character, we can understand why in Table III the overlap of the $M(CO)_3$ hy with the main-group probe orbital, which is a mixture of 2s and $2p_z$, is greater than that of $M(C_6H_6)$ hy. The more p character in the coupling lone pair, the greater the differential. Conversely, if the donor orbital is mainly s (for instance, a hydride) $M(CO)_3$ and $M(C_6H_6)$ should possess similar $\sigma$-bonding capabilities.

While the group overlaps of Table III indicate that an $M(CO)_3$ fragment should have a somewhat stronger $\sigma$ interaction than $M(C_6H_6)$, we were concerned that the conclusion rested on overlap differentials involving metal 4s and 4p orbitals. The shape of these orbitals is uncertain, the particular Slater exponent assumed by us being little more than a guess. We therefore repeated the $ML_n$-probe calculations with different 4s and 4p exponents. These were judged appropriate for M = Ni (see Appendix) and gave considerably more contracted 4s and 4p functions. The group orbital overlaps of Table III in fact are sensitive to the metal wave function, for the trends noted were reversed by a little. We are not left with a definitive comparison of the $M(CO)_3$ and M(arene) $\sigma$-bonding capability—from the theoretical point of view the fragments appear roughly equivalent.

In contrast to the above discussion it is $M(C_6H_6)$ that should be more effective at bonding with another metal. At the distances of 2.5–3.0 Å characteristic of metal–metal bonding the primary overlap is between the diffuse s and p orbitals of the metal. The noded and relatively contracted d functions provide a poor overlap with other metal d orbitals or s and p functions, as may be seen in Table IV. The $M(CO)_3$ fragment, with its admixture of $z^2$, should be less effective at bonding with another metal than $M(C_6H_6)$. We also note that the trends in interaction with a metal probe are insensitive to the choice of metal wave function.

In evaluating the $\pi$ interactions the important points are that *xz* and *yz* in $M(CO)_3$ are both more delocalized to the $(CO)_3$ and more hybridized with metal *x* and *y* than is the case in $M(C_6H_6)$. The greater delocalization away from the metal is responsible for the smaller $M(CO)_3$ $\pi$ overlap with a main-group probe. The hybridization, on the other hand, enhances overlap with a metal atom center.

The conclusions which we obtain from the preceding laborious discussion are the following: *For coupling with another metal probe $M(C_6H_6)$ definitely has a stronger $\sigma$ interaction, but $M(CO)_3$ is better at $\pi$ bonding.* The $\sigma$ effect appears to be dominant. For main-group probes our comparison of $\sigma$ and $\pi$ interactions of $M(CO)_3$ and $M(C_6H_6)$ is inconclusive. Given this situation for the overlap factor, one could fall back on the role of the residual charge on the metal. This would imply that an $M(CO)_3$ group is a worse $\pi$ donor and better $\sigma$ acceptor than $M(C_6H_6)$.

Our next concern is to compare these conclusions with the experimental evidence that is available. A comparison of $M(CO)_3$ and $M(C_6H_6)$ is relatively restrictive, for indeed the most common replacement is of $M(CO)_3$ by M′($\eta^5$-cyclopentadienyl), M′(Cp), **8**. There is a slight problem with an analysis of the latter two systems due to the fact that in order to obtain a truly isoelectronic interchange one must change the transition metal as well, from M to M′ = metal with atomic number M + 1. For instance interchangeable pairs are $Fe(CO)_3$ and $Co(C_5H_5)$; and $Co(CO)_3$ and $Ni(C_5H_5)$. We prefer to have only one part of the system change, not both the metal and the ligands. Fortunately the symmetry properties and overlaps of cyclopentadienyl ligand are very similar to those of benzene. This allows us to make an analysis of **1** and **2**, where the metal atom is the same. At selected places in our discussion we will point to the possible perturbation caused by changing the metal.

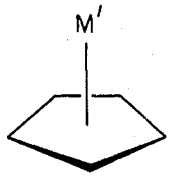


**8**

**Structural Information on Matched $M(CO)_3$, $M(C_6H_6)$, and M(Cp) Complexes**

An examination of the experimental evidence relevant to our theoretical conclusions must be prefaced by three general comments. First, there is little thermochemical information on these molecules.[10] We must draw whatever conclusions we can concerning the differential bonding from the results of structural studies. Some indirect information may be forthcoming from spectroscopic studies, but we have not attempted to review it. Second, despite the generality of the replacement of $M(CO)_3$ by $M(C_6H_6)$ or M'(Cp) there are relatively few structures to compare. It may be that the assurance that has built up that such groupings are indeed replaceable has operated against the allocation of precious time to carry out several structural studies. Third, for the few structures that we have we are put in the uncomfortable position of comparing structural investigations often of disparate quality. A few accurate structural studies would quickly clear up the questions posed by the replacement, but for the present we must ask the reader to bear with us as we review the evidence that is available.

For metal–metal interactions we have several pertinent examples. The structure of phenylmethinyltricobalt hexacarbonyl,[11] **9**, offers an interesting internal comparison of

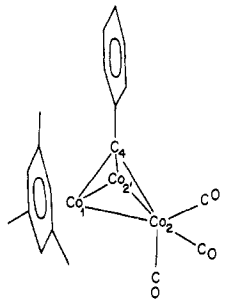

9

$Co_1$–$Co_2$ = 2.44 Å
$Co_2$–$Co_2'$ = 2.48 Å
$Co_1$–$C_4$ = 1.87 Å
$Co_2$–$C_4$ = 1.90 Å

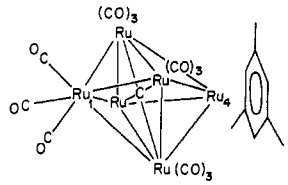

10

$Ru_1$–Ru = 2.86, 2.90 Å
$Ru_4$–Ru = 2.85, 2.86 Å
$Ru_1$–C = 2.12 Å
$Ru_4$–C = 1.88 Å

$Co(CO)_3$ and Co(mesitylene). Note that the bonds with the Co(mesitylene) fragment are consistently shorter, as expected. A related comparison of $Co_4(CO)_{12}$[12] with $Co_3(CO)_9$(arene)[13] is hampered by crystallographic problems due to disorder in the crystal of the former molecule. A ruthenium carbonyl carbide cluster,[14] **10**, also shows shorter Ru(arene) to C and Ru distances.

Another metal–metal comparison is available from the acetylene complex structures **11**[15] and **12**.[16] The Co structure

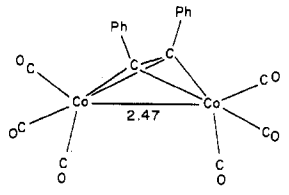

11

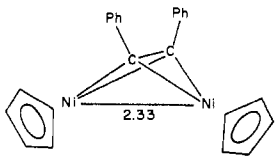

12

is an early one, with a large *R* factor. The Co–Co distance is longer.

The series **13**,[17] **14**,[18] and **15**[19] provides a stepwise replacement of $(CO)_3Co$ by CpNi. The metal–metal separation decreases along the series.

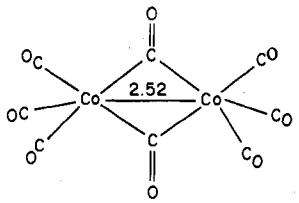

13

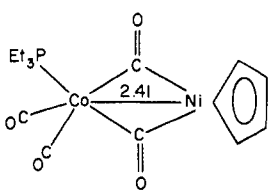

14

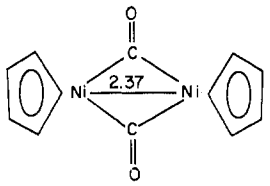

15

In structures **16**[20] and **17**[21] there is a double fragment

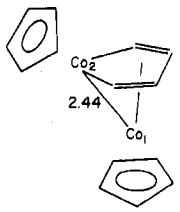

16

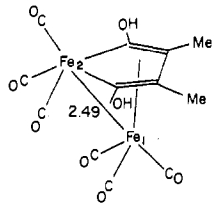

17

substitution. As expected, the CpCo–CoCp distance is shorter than $(CO)_3Fe$–$Fe(CO)_3$. The average $Co_1$–C($MC_4$ ring) distance of 2.03 Å is shorter than the corresponding Fe–C distance of 2.13 Å. Also the average $Co_2$–C distance in the $MC_4$ cycle, 1.87 Å, is shorter than the $Fe_2$–C distance of 1.94 Å. The shorter CpCo–main group bond lengths are not in agreement with our expectations, and perhaps this is the appropriate place to face up to the problems of interpretation caused by the cyclopentadienyl ligand.

The symmetries, distances and overlaps of $C_5H_5$ and $C_6H_6$ fragments are very similar and, were it not for the different metal atom that must be coupled to these to achieve isoelectronic fragments, the donor and acceptor orbitals of $C_6H_6M$ and CpM' would be nearly identical. The difference between M and M' is one of atomic number and oxidation state—Fe(0) and Co(I); Co(0) and Ni(I). The effect of the increased oxidation state is in principle felt in two ways: (1) through an increased splitting of metal s and d levels, with a corollary decrease in hybridization, and (2) through a contraction in the size of the atom.[22] Of course, electroneutrality to some extent tempers the distinction implied by the oxidation-state formalism. Nevertheless, one would expect a $Ni^{II}$–L distance to be inherently shorter than a $Co^{I}$–L separation. Whenever we contrast the bonding capabilities of $(CO)_3Co$ with CpNi, we will have to remember that any electronic effects that we postulate are operating on top of this background.

The nitrosyl ligand serves as a simple main-group probe in $(CO)_3Co(NO)$ and CpNi(NO). An electron diffraction structure is available for the former,[23] while for the latter we have a microwave structure[24a] as well as an electron diffraction structure.[24b] If the NO is viewed as $NO^+$, these are $d^{10}$ systems. The NO group is a good $\sigma$ donor and an excellent $\pi$ acceptor. The Co–N distance is 1.67 Å and Ni–N is 1.63 Å, which again may be due, at least in part, to a change in oxidation state.

The structures of tetrakis(trifluoromethyl)cyclopentadienone complexes with $Fe(CO)_3$ and CoCp are available.[25] The structural type is shown in **18**. The two structures show

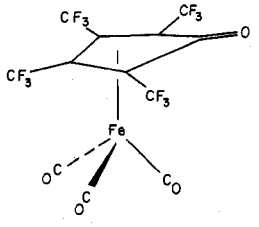

18

similar angles of bending up of the carbonyl group and metal–ring distances and a somewhat longer set of C–C distances in the cyclopentadienone ring for the CoCp complex. But the structural parameters are not of high accuracy, so that little significance can be attached to the variations.

As a final structural comparison we cite the clusters $(CO)_9Fe_3S_2$, $(CO)_9Fe_3Se_2$, $Cp_3Co_3S_2$, and $Cp_3Co_3S_2^+$. The first two low-spin compounds possess an open $C_{2v}$ structure,[26,27] **19**, with one Fe–Fe distance much longer than the other two.

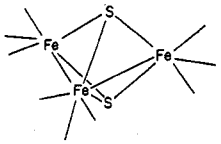

19

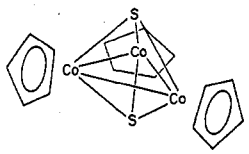

20

$Cp_3Co_3S_2$, which is a triplet at room temperature,[28,29] is a closed $D_{3h}$ structure,[28] **20**. Its cation is slightly distorted to a $C_{2v}$ geometry with one Co–Co distance slightly shorter than the other two. A qualitative MO scheme[29] rationalizes perfectly well the geometrical distortions in this system. In a $D_{3h}$ geometry two electrons occupy an antibonding e' orbital.[30] A distortion to $C_{2v}$ breaks the degeneracy. It is understandable that a high-spin two-electron system would maintain the $D_{3h}$ geometry, while a low-spin state would distort.

The general picture that emerges from an examination of these structures is one of agreement with our theoretical conclusions on stronger metal–metal bonding with an M-$(C_6H_6)$ or M'$(C_5H_5)$ fragment. For the metal–main group bonding the theoretical result was not clear, and the experimental picture seems to be dominated by oxidation-state arguments.

**Pyramidality Deformations in $M(CH)_n$ and $M(CO)_3$**

In this section we discuss two small but interesting distortions in $M(CH)_n$- and $M(CO)_3$-containing structures. The first of these concerns the noncoplanarity of the cyclopolyene hydrogens with the carbon plane, and the second deals with the variable pyramidality of the $(CO)_3$ grouping.

Accurate structural investigations show that when a cyclopolyene is coordinated to a transition metal center, the hydrogens or other ring substituents may be bent toward or away from the metal. In examining such structures we exclude highly unsymmetrically substituted molecules and complexes in which not all of the $(CR)_n$ centers are coordinated to the metal. A significant set of distortions remain. Let us define the deformation by an angle $\theta$ between the C–R axis and the ring plane, as shown in **21**. Positive $\theta$ will correspond to

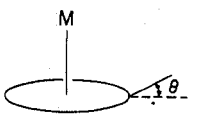

21

bending toward the metal; negative $\theta$, to bending away.

Table V. EH Optimized $\theta$ in a Series of $M(CH)_n$ Fragments

| Fragment | Co- $(C_3H_3)$ | Fe- $(C_4H_4)$ | Mn- $(C_5H_5)$ | Cr- $(C_6H_6)$ | V- $(C_7H_7)$ | Ti- $(C_8H_8)$ |
|---|---|---|---|---|---|---|
| Optimal $\theta$ | −26° | −6° | 0° | 3° | 9° | 13° |

Let us first consider coordinated benzene rings. A neutron and crystal diffraction study of benzenechromium tricarbonyl[31] gives an average bending angle of +1.7°. Similar positive $\theta$ deformations are observed for bis(benzene)chromium,[32,33] but negative $\theta$ deformations, away from the metal, have been found for hexamethylbenzenechromium tricarbonyl[34] and the $\eta^6$ ring in bis(hexamethylbenzene)ruthenium.[35] The entire range of deformations is small, and no one would be surprised if the observed distortions were a consequence of crystal packing forces. Nevertheless, it is interesting to study the problem theoretically—there is no constraint holding the cyclopolyene substituents in the carbon plane.

An optimization of $\theta$ in a $d^6$ $Cr(C_6H_6)$ fragment yields an energy minimum for hydrogens bent toward the metal by 3.2°. The bending can be traced to an $e_1$ orbital, the in-phase combination of metal $xz$ and $yz$ with the benzene $e_{1g}$ orbital. The shape of one component of this orbital for a planar benzene is illustrated in **22**. The reason that this orbital

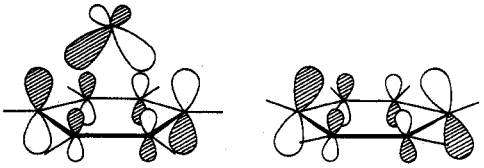

22 23

combination is stabilized for a distorted benzene with hydrogens bent toward the metal is that the metal–benzene overlap is increased by such a distortion. Bending the hydrogens up reorients[36] the benzene MO's in such a way that the $e_{1g}$ orbital ($e_1$ in the reduced $C_{6v}$ symmetry) lobes tilt to point in at the metal, **23**. This orbital deformation increases the overlap with metal $xz$ and $yz$. A similar explanation in terms of ring p orbital reorientation for better M–ring bonding has been given earlier by Kettle.[37]

If we accept this explanation for the small positive $\theta$ deformation, then we must attribute the negative $\theta$ distortions in hexamethylbenzenes to steric effects. The overall credibility of our rationalization is however enhanced by surveying the analogous distortions as a function of cyclopolyene ring size. If the crucial bonding effect is the $(xz, yz)$–$e_1$ interaction, then for large rings overlap will be maximized by a tilting in of the $e_1$ $\pi$ orbitals (as shown in **23**), and $\theta$ would be positive. But for small rings the ligand $\pi$ set should tilt out, as in **24**, to

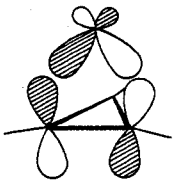

24

increase overlap with $xz$ and $yz$, and the optimum $\theta$ should be negative. Extended Hückel optimizations of $\theta$ on a series of $M(CH)_n$ fragments lend support to this argument. A tabulation of these results is given in Table V. There is a continuous trend of the hydrogens approaching the metal as the rings increase in size.

What is known experimentally for various ring sizes is the following: $\theta$ is an average +4.1° for the methyl groups of bis(1,3,5,7-tetramethylcyclooctatetraenyl)uranium.[38] A better example perhaps is to be found in the structure of $[C_8H_8$-

$TiCl]_4$, where the hydrogens in each $C_8H_8Ti$ unit are displaced toward the Ti.[38] In ferrocene $\theta$ is positive;[40] in $(C_5Me_5)Rh(dba)$[41] and in $(C_5Me_5)Fe(CO)_2SO_2CH_2CH{=}CHPh$,[42] negative. In less symmetrical ferrocenes there appears to be no significant trend, with $\theta$ being sometimes positive and sometimes negative.[43]

Substituents on complexed cyclobutadienes consistently bend away from the metal. $\theta$ is $-10.8°$ in $(C_4Ph_4)Fe(CO)_3$[44] and also negative in two less symmetrical systems: $[C_4Me_4NiCl]_2$[45] and $[C_4Ph_2(t\text{-}Bu)_2]_2Fe_2(CO)_3$.[46]

Complexed cyclopropenyl groups show a significant bending of ring substituents away from the metal. Thus the average bending angle is $-20°$ in $CpNi(C_3Ph_3)$[47] and $-19°$ in $Cl(py)_2Ni(C_3Ph_3)$.[48]

Our analysis further predicts that in $M(CH)_n$ complexes the crossover between positive and negative $\theta$, which in complexes of the first transition series appears to occur at $n \simeq 5$, should shift to larger $n$ for M in the second or third transition series. The corresponding metal $xz$ and $yz$ orbitals are more diffuse. For a large ring they require less reorientation for maximal overlap.

Parenthetically we might mention that the typical bending away of substituents on a complexed ethylene may be readily understood as a limiting case for application of the arguments cited above.

Let us discuss a different deformation, the modification of the pyramidality of the $M(CO)_3$ fragment. A measure of this is the angle $\phi$ in **25**. As discussed earlier,[4] the $a_1$ and e (hy,

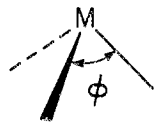


25

$xz$, $yz$ in Figure 1) orbitals of the $M(CO)_3$ fragment will both decrease in energy with increasing $\phi$, i.e., the more planar the $M(CO)_3$. In a quasi-tetrahedral $d^{10}$ system $(CO)_3ML$ $xz$ and $yz$ are filled and play a donor role. It follows that the stronger the $\pi$-acceptor capability of L (and the worse its $\sigma$-donor function) the more pyramidal the $M(CO)_3$ grouping. For related $(PR_3)_3ML$ systems the experimental evidence is in accord with this.[49]

For a quasi-octahedral $d^6$ system $(CO)_3ML_3$ hy, $xz$, and $yz$ are all empty and act as acceptor orbitals for the incoming donor orbitals of three L groups. The stronger the donating capability of L the less pyramidal should be the $M(CO)_3$ fragment. The same should hold true if $L_3$ is replaced by a cyclopolyene, $(CH)_n^{6-n}$. In Figure 3 we note that the energy of the $\pi$ orbital (and hence the donor strength) rises with decreasing $n$. Therefore the pyramidality of the carbonyl cone in $(CH)_nM(CO)_3$ is expected to decrease with $n$. Experimental confirmation of this is found in the structures $C_6H_6Cr(CO)_3$,[31] $C_5H_5Mn(CO)_3$,[50] and $C_4Me_4Fe(CO)_3$[44] where the average $\phi$ is 88, 92, and 97°, respectively. A comparison of $C_6H_3(NO_2)_3Cr(CO)_3$ (average $\phi = 89°$)[51] with $C_6H_6Cr(CO)_3$, however, seems to indicate that $\phi$ is relatively insensitive to substituents on the ring.

**Acknowledgment**. Our work was generously supported by the National Science Foundation, the Advanced Research Projects Agency through the Materials Science Center at Cornell University, and the Scientific Affairs Division of NATO. The stay at Cornell of M.E. (from the Institute of Organic Chemistry, Bucharest, Romania) was made possible by a grant from the Committee on International Exchange of Persons (Senior Fulbright–Hays Program). We are grateful to the members of our research group for their valuable contributions to the discussion.

## Appendix

Extended Hückel calculations[52] were carried out using the following geometries and atom parameters. $M(CO)_3$ had the idealized octahedral fragment geometry with angle CMC = 90°. Bond distances were M–C = 1.80 Å and C–O = 1.13 Å. $M(CH)_n$ bond distances were M–C = 2.19 Å, C–C = 1.40 Å, C–H = 1.08 Å. The ring was kept planar with M above its center. NO was set at 1.71 and 2.10 Å from the metal fragments with N–O = 1.17 Å. $MH_3$ was calculated at 2.90 Å from the metal with angle HMH = 90° and M–H = 1.5 Å. Table VI summarizes the extended Hückel parameters used.

**Table VI.** Extended Hückel Parameters for Nonmetals

| Orbital | Slater exp | $H_{ii}$, eV | Orbital | Slater exp | $H_{ii}$, eV |
|---|---|---|---|---|---|
| H 1s | 1.30 | −13.60 | N 2p | 1.950 | −13.40 |
| C 2s | 1.625 | −21.40 | O 2s | 2.275 | −32.30 |
| C 2p | 1.625 | −11.40 | O 2p | 2.275 | −14.80 |
| N 2s | 1.950 | −26.00 | | | |

**Table VII.** Extended Hückel Parameters for Metals

| Orbital | Slater exp 1 | $H_{ii}$, eV | Slater exp 2 | Coeff 1 | Coeff 2 |
|---|---|---|---|---|---|
| Mn 4s | 0.97 | −9.75 | | | |
| Mn 4p | 0.97 | −5.89 | | | |
| Mn 3d | 5.15 | −11.67 | 1.7 | 0.5139 | 0.6929 |
| Ni 4s | 1.825 | −9.75 | | | |
| Ni 4p | 1.125 | −5.89 | | | |
| Ni 3d | 5.75 | −11.67 | 2.0 | 0.5683 | 0.6292 |

To span a range of metal wave functions we used the exponents of Mn and Ni, keeping the $H_{ii}$ the same in both cases (see Table VII). The metal d functions were taken as double-$\zeta$ functions.[53] In the series of calculations, such as Figures 2 and 3 and Table V, the metal parameters were constant. Only the number of electrons changed.

## References and Notes

(1) Throughout this paper we use the abbreviated notation $z^2$ for $d_{z^2}$, $z$ for $p_z$, etc.
(2) The arrangement of three carbon monoxides into the geometry they occupy in an $M(CO)_3$ fragment introduces CO–CO overlaps large enough to produce a significant mixing and consequent reorientation of all orbitals of the carbonyls—$\sigma$, $\pi$, $\pi^*$, $\sigma^*$. The block of low-lying unfilled orbitals $a_1 + a_2 + 2$ e is still recognizable as primarily $\pi^*$.
(3) The importance of M–ring $\sigma$ overlaps has been previously stressed by D. G. Carroll and S. P. McGlynn, *Inorg. Chem.*, **7**, 1285 (1968).
(4) M. Elian and R. Hoffmann, *Inorg. Chem.*, **14**, 1058 (1975).
(5) The methodology is described in R. Hoffmann, *Acc. Chem. Res.*, **4**, 1 (1971); L. Libit and R. Hoffmann, *J. Am. Chem. Soc.*, **96**, 1370 (1974).
(6) Much of the chemistry as well as the structures of these complexes can be found in the following surveys: M. L. H. Green, "Organometallic Compounds. The Transition Elements", 3d ed, Methuen, London, 1968; P. J. Wheatley, *Perspect. Struct. Chem.*, **1**, 1 (1967).
(7) Theoretical analyses of $M(CH)_n$ interactions are given in the following: (a) L. E. Orgel, "An Introduction to Transition Metal Chemistry", 2d ed, Wiley, New York, N.Y., 1966; (b) D. A. Brown, *J. Inorg. Nucl. Chem.*, **10**, 39 (1959); see also D. A. Brown and R. M. Rawlinson, *J. Chem. Soc. A*, 1534 (1969); D. A. Brown, N. J. Fitzpatrick, and N. J. Mathews, *J. Organomet. Chem.*, **88**, C27 (1975); (c) R. D. Fischer, *Theor. Chim. Acta*, **1**, 418 (1963).
(8) The $M(CH)_n$ orbitals are very nicely analyzed in the context of a photoelectron study of some sandwich complexes by S. Evans, J. C. Green, S. E. Jackson, and B. Higginson, *J. Chem. Soc., Dalton Trans.*, 304 (1974), and in the context of both reactivity and photoelectron spectroscopy by C. J. Groenenboom, H. J. de Liefde Meijer, and F. Jellinek, *Recl. Trav. Chim. Pays-Bas*, **93**, 6 (1974); *J. Organomet. Chem.*, **69**, 235 (1974); C. J. Groenenboom, H. J. de Liefde Meijer, F. Jellinek, and A. Oskam, *ibid.*, **97**, 73 (1975); M. Vliek, C. J. Groenenboom, H. J. de Liefde Meijer, and F. Jellinek, *ibid.*, **97**, 67 (1975).
(9) This distance is between the observed M–N distances in $Co(CO)_3NO$ and CpNiNO. Being as short as it is, it may not be typical of $ML_n$–main group interaction. With this in mind we repeated our calculations for the NO probe, but placing it 2.1 Å away from the metal. All conclusions were qualitatively similar.
(10) See J. D. Cox and G. Pilcher "Thermochemistry of Organic and Organometallic Compounds", Academic Press, New York, N.Y., 1970. Some recent measurements on the strength of arene–$Cr(CO)_3$ bonds are summarized by F. A. Adedeji, D. L. S. Brown, J. A. Connor, M. L. Leung,

I. M. Paz-Andrade, and H. A. Skinner, *J. Organomet. Chem.*, **97**, 221 (1975).
(11) R. J. Dellaca and B. R. Penfold, *Inorg. Chem.*, **11**, 1855 (1972); M. D. Brice, R. J. Dellaca, B. R. Penfold, and J. L. Spencer, *Chem. Commun.*, 72 (1971).
(12) C. H. Wei, *Inorg. Chem.*, **8**, 2384 (1969).
(13) P. H. Bird and A. R. Fraser, *J. Organomet. Chem.*, **73**, 103 (1974).
(14) R. Mason and W. R. Robinson, *Chem. Commun.*, 468 (1968).
(15) W. G. Sly, *J. Am. Chem. Soc.*, **81**, 18 (1959).
(16) O. S. Mills and B. W. Shaw, *J. Organomet. Chem.*, **11**, 595 (1968).
(17) G. G. Sumner, H. P. Klug, and L. E. Alexander, *Acta Crystallogr.*, **17**, 732 (1964).
(18) F. S. Stephens, *J. Chem. Soc., Dalton Trans.*, 1067 (1974).
(19) J. P. Nice, Ph.D. Thesis, University of Manchester, 1966.
(20) O. S. Mills, private communication.
(21) A. A. Hock and O. S. Mills, *Acta Crystallogr.*, **14**, 139 (1961).
(22) In this context see the discussion of covalent radii by M. R. Churchill, *Perspect. Struct. Chem.*, **3**, 91 (1970).
(23) K. Hedberg, Oregon State University, private communication. There is an older structure by L. O. Brockaway and J. S. Anderson, *Trans. Faraday Soc.*, **33**, 1233 (1937).
(24) (a) A. P. Cox and A. H. Brittain, *Trans. Faraday Soc.*, **66**, 557 (1970); (b) I. A. Ronova, N. V. Alekseeva, N. N. Veniaminov, and M. A. Kravers, *Zh. Strukt. Khim.*, **16**, 476 (1975).
(25) (a) N. A. Bailey and R. Mason, *Acta Crystallogr.*, **21**, 652 (1966); (b) M. Gerloch and R. Mason, *Proc. R. Soc. London, Ser. A*, **279**, 170 (1964).
(26) C. H. Wei and L. F. Dahl, *Inorg. Chem.*, **4**, 493 (1965).
(27) L. F. Dahl and P. W. Sutton, *Inorg. Chem.*, **2**, 1067 (1963).
(28) (a) S. Otsuka, A. Nakamura, and T. Yoshida, *Inorg. Chem.*, 7, 261 (1968); (b) M. Sorai, A. Kosaki, H. Suga, S. Seki, T. Yoshida, and S. Otsuka, *Bull. Chem. Soc. Jpn.*, **44**, 2364 (1971).
(29) P. D. Frisch and L. F. Dahl, *J. Am. Chem. Soc.*, **94**, 5082 (1972).
(30) Our extended Hückel calculations on $(CO)_9M_3S_2$ and $Cp_3M_3S_2$ concur in this assignment.
(31) B. Rees and P. Coppens, *Acta Crystallogr., Sect. B*, **29**, 2515 (1973).
(32) A. Haaland, *Acta Chem. Scand.*, **19**, 41 (1965).
(33) E. Keulen and F. Jellinek, *J. Organomet. Chem.*, **5**, 490 (1966).
(34) M. F. Bailey and L. F. Dahl, *Inorg. Chem.*, **4**, 1298 (1965).
(35) G. Huttner and S. Lange, *Acta Crystallogr., Sect. B*, **28**, 2049 (1972).
(36) This is accomplished by $\sigma$–$\pi$ mixing of what were $e_{1g}$ and $e_{1u}$ orbitals in benzene. For illustrations of these orbitals see W. L. Jorgensen and L. Salem, "The Organic Chemist's Book of Orbitals", Academic Press, New York, N.Y., 1973, pp 257–259.
(37) S. F. A. Kettle, *Inorg. Chim. Acta*, **1**, 303 (1967).
(38) K. O. Hodgson and K. N. Raymond, *Inorg. Chem.*, **12**, 458 (1973).
(39) H. R. van der Wal, F. Overzet, H. O. van Oven, J. L. de Boer, H. J. de Liefde Meijer, and F. Jellinek, *J. Organomet. Chem.*, **92**, 329 (1975).
(40) R. K. Bohn and A. Haaland, *J. Organomet. Chem.*, **5**, 470 (1966).
(41) J. A. Ibers, *J. Organomet. Chem.*, **73**, 389 (1974).
(42) M. R. Churchill and J. Wormald, *Inorg. Chem.*, **10**, 572 (1971).
(43) See references surveyed in ref 38.
(44) R. P. Dodge and V. Schomaker, *Acta Crystallogr.*, **18**, 614 (1965).
(45) J. D. Dunitz, H. C. Mez, O. S. Mills, and H. M. M. Shearer, *Helv. Chim. Acta*, **45**, 647 (1962).
(46) S. Murahashi, T. Mizoguchi, T. Hosokawa, I. Moritani, Y. Kai, M. Kohara, N. Yasuoka, and N. Kasai, *J. Chem. Soc., Chem. Commun.*, 563 (1974).
(47) M. D. Rausch, R. M. Tuggle, and D. L. Weaver, *J. Am. Chem. Soc.*, **92**, 4981 (1970); R. M. Tuggle and D. L. Weaver, *Inorg. Chem.*, **10**, 1504 (1971).
(48) R. M. Tuggle and D. L. Weaver, *Inorg. Chem.*, **10**, 2599 (1971).
(49) See the discussion on p 1069 of ref 4.
(50) A. F. Berndt and R. E. Marsh, *Acta Crystallogr.*, **16**, 118 (1963).
(51) O. L. Carter, A. T. McPhail, and G. A. Sim, *J. Chem. Soc. A*, 822 (1966).
(52) R. Hoffmann, *J. Chem. Phys.*, **39**, 1397 (1963); R. Hoffmann and W. N. Lipscomb, *ibid.*, **36**, 2179, 3489 (1962); **37**, 2872 (1962).
(53) J. W. Richardson, W. C. Nieuwpoort, R. R. Powell, and W. F. Edgell, *J. Chem. Phys.*, **36**, 1057 (1962).

Contribution from the Department of Chemistry, Columbia University, New York, New York 10027

# Structural Determinations of Four Mono- and Binuclear Tertiary Phosphine and Arsine Complexes of Copper(I) Chloride

J. T. GILL, J. J. MAYERLE, P. S. WELCKER, D. F. LEWIS, D. A. UCKO, D. J. BARTON, D. STOWENS, and S. J. LIPPARD*

*Received September 15, 1975* AIC50683L

The structure of $[(C_6H_5)_3P]_3CuCl$ has been determined by x-ray diffraction. The compound crystallizes in the trigonal space group $P\bar{3}$, with unit cell dimensions $a$ = 19.2775 (14) Å and $c$ = 10.4720 (9) Å, and $Z$ = 3. A crystallographic threefold rotation axis passes through the Cu–Cl bond. Some important bond distances and angles are Cu–Cl(av) = 2.34 (2) Å, Cu–P(av) = 2.351 (4) Å, Cl–Cu–P(av) = 109.1 (7)°, and P–Cu–P(av) = 109.8 (7)°. The compound $[(C_6H_5)_2(CH_3)P]_3CuCl$ crystallizes in the orthorhombic space group $Pn2_1a$, with $Z$ = 4 and cell constants $a$ = 20.229 (14) Å, $b$ = 17.180 (10) Å, and $c$ = 10.309 (5) Å. The molecular geometry is approximately tetrahedral. The rotational conformation about the three Cu–P bonds creates a sterically favorable pocket for the chlorine atom. Some distances and angles are Cu–Cl = 2.366 (4) Å, Cu–P(av) = 2.289 (6) Å, Cl–Cu–P(av) = 103 (2)°, and P–Cu–P = 108.3 (1), 117.7 (1), 118.1 (1)°. The compound $\{[(C_6H_5)(CH_3)_2As]_2CuCl\}_2$ crystallizes in the monoclinic space group $P2_1/n$, with unit cell parameters $a$ = 9.888 (3) Å, $b$ = 17.082 (5) Å, $c$ = 11.277 (6) Å, and $\beta$ = 94.11 (2)°, and $Z$ = 2 (dimers). The molecule is a dichloride-bridged dimer having two pseudotetrahedral copper atoms related by an inversion center. Selected distances and angles are Cu–Cl(av) = 2.380 (6) Å, Cu–As(av) = 2.36 (1) Å, As–Cu–As = 118.00 (9)°, Cl–Cu–Cl = 100.9 (1)°, and Cl–Cu–As = 100.7 (1), 105.3 (1), 115.1 (1), 115.8 (1)°. Finally, $[(C_6H_5)_3P]_3Cu_2Cl_2\cdot C_6H_6$ is triclinic, space group $P\bar{1}$, with cell constants $a$ = 12.307 (5) Å, $b$ = 18.722 (9) Å, $c$ = 13.574 (5) Å, $\alpha$ = 117.174 (13)°, $\beta$ = 73.794 (6)°, and $\gamma$ = 107.554 (12)°, and $Z$ = 2. Each molecule contains the di-$\mu$-chloro-dicopper(I) core with two triphenylphosphine ligands bonded to one copper atom and one triphenylphosphine ligand bonded to the other copper atom. The result is a binuclear compound containing both three- and pseudotetrahedral four-coordinate copper. The mean copper–chlorine distance of 2.46 (2) Å and copper–phosphorus distance of 2.260 (5) Å in the latter are significantly longer than the respective values of 2.28 (2) and 2.183 (3) Å in the former. Selected interbond angles are Cl–Cu–P(trig) = 123.63 (9), 134.74 (8)°, Cl–Cu–Cl(trig) = 101.63 (9)°, P–Cu–P(tet) = 130.40 (8)°, Cl–Cu–Cl(tet) = 91.57 (8)°, and Cu–Cl–Cu(av) = 82.9 (2)°. Geometries of the four compounds are discussed in detail and compared to those of other $L_m(CuX)_n$ complexes, where L = tertiary phosphine or arsine and X = coordinating anion.

## Introduction

Until 1967, only two x-ray structural studies of tertiary monodentate group 5 ligand–copper(I) complexes had been reported. These were Wells' investigation of $[(C_2H_5)_3As\text{-}CuI]_4$[1] and the study of $[(CH_3)_3P(C_6H_5C{\equiv}C)Cu]_4$ by Corfield and Shearer.[2] The x-ray structure determination of $[(C_6H_5)_3P]_2CuBH_4$[3] in that year, however, presaged a strong new interest in these compounds, not only in our laboratory but in several others as well. Numerous stoichiometries and structures are now known for $L_m(CuX)_n$ complexes, where L